CTP-TAMU-35-00

Prospect for Searches for Gluinos and Squarks at a Tevatron Tripler

V. Krutelyov[1], R. Arnowitt[2], B. Dutta[2],

T. Kamon[1], P. McIntyre[1], Y. Santoso[2]

[1] *Department of Physics, Texas A&M University, College Station, TX 77843-4242,*

[2] *Center for Theoretical Physics, Department of Physics, Texas A&M University, College Station, TX 77843-4242.*

(November, 2000)

Abstract

We examine the discovery potential for SUSY new physics at a $p\bar{p}$ collider upgrade of Tevatron with $\sqrt{s} = 5.4$ TeV and luminosity $\mathcal{L} \simeq 4 \times 10^{32}$ cm^{-2}s^{-1} (the Tripler). We consider the reach for gluinos ($\tilde{g}$) and squarks ($\tilde{q}$) using the experimental signatures with large missing transverse energy ($\not\!\!E_T$) of jets + $\not\!\!E_T$ and 1ℓ + jets + $\not\!\!E_T$ (where ℓ=electron or muon) within the framework of minimal supergravity. The Tripler's strongest reach for the gluino is 1060 GeV for the jets + $\not\!\!E_T$ channel and 1140 GeV for the 1ℓ + jets + $\not\!\!E_T$ channel for 30 fb^{-1} of integrated luminosity (approximately two years running time). This is to be compared with the Tevatron where the reach is 440(460) GeV in the jets + $\not\!\!E_T$ channel for 15(30) fb^{-1} of integrated luminosity.

I. INTRODUCTION

The Tripler [1] is a proposed energy upgrade of the Tevatron, in which its ring of 4 Tesla NbTi superconducting magnets would be replaced by a ring of 12 Tesla Nb_3Sn magnets. Thanks to improvements in Nb_3Sn technology and in dipole design methodology, it is now possible to extend dipole fields up to and beyond 12 Tesla. Prototype magnets are being developed using several different methodologies at Brookhaven National Lab [2], Fermilab [3], Lawrence Berkeley National Lab [4], and Texas A&M University [5].

The rationale for the Tripler is that the upgrade opens an energy window in which the particles of the Higgs sector and new physics are expected to be produced in a mass range of $\lesssim 1$ TeV. The Tripler furthermore accesses this energy window primarily through quark-antiquark annihilation and gluon fusion, whereas the Large Hadron Collider (LHC) will access a similar window primarily through gluon fusion and gluon-quark/quark-quark interaction. The proposed Next Linear Collider (NLC) with its center-of-mass (c.m.) energy of 500 GeV [6] will access a limited energy window through e^+e^- annihilation, but with more precise measurements of the parameters of theories. Complimentarity has often proved vital in understanding new phenomena at the high-energy frontier. The Tripler would use the existing tunnel, existing $\bar{p}$ source and injector accelerators, and existing detectors CDF and DØ with minimal changes. With a luminosity of about 4×10^{32} cm^{-2}s^{-1} and live time of 2×10^7 sec/year, the Tripler would deliver about 8 fb^{-1}/year for each detector [1].

The present paper is concerned with evaluating the reach of the Tripler for new physics. Reference [7] analyzed the signals for the Standard Model (SM) Higgs boson at the Tripler and compared them with those at the LHC [8,9]. It is remarkable that the Tripler can discover a Higgs boson up to 680 (600) GeV mass with 40 (10) fb^{-1} of integrated luminosity, which is close to the triviality upper bound of 710 GeV [10]. A light Higgs boson ($\lesssim 130$ GeV) would be accessible via WWH coupling with 7.5 fb^{-1} at the Tripler, while its production at the LHC proceeds predominantly via processes involving Yukawa couplings.

Another important benchmark for the physics is the potential to discover the particles of

supersymmetry (SUSY) [11]. There have been extensive analyses of the discovery potential for SUSY particles, based on minimal spergravity (mSUGRA) model [12] or minimal Supersymmetric Standard Model (MSSM), at the Tevatron [13–23] and at the LHC [8,24]. In the Tripler case, SUSY studies on $p\overline{p} \to 3\ell + \not\!\!E_T + X$ (dominantly from $\tilde{\chi}_1^{\pm}\tilde{\chi}_2^0$ production) and $p\overline{p} \to \ell^{\pm}\ell^{\pm}$ + jets + $\not\!\!E_T$ (dominantly from $\tilde{g}\tilde{g}/\tilde{g}\tilde{q}$ production) have been carried out in Ref. [7]. In this paper we present a comparative study of the discovery reaches for gluinos and squarks with large missing transverse energy ($\not\!\!E_T$). We examine the signals from jets + $\not\!\!E_T$ and 1ℓ + jets + $\not\!\!E_T$ (ℓ=electron or muon) at the Tripler and compare these signals at the Tevatron.

II. MSUGRA MODEL

To test the reach of the Tripler for gluinos ($\tilde{g}$) and squarks ($\tilde{q}$), we consider SUSY models for which grand unification of the gauge coupling constants occur at a GUT scale $M_G \equiv 2\times 10^{16}$ GeV. These models are consistent with the LEP measurements of $\alpha_i(i$=1,2,3) at the electroweak scale M_Z when the renormalization group equations (RGE) are used to run the α_i up to M_G, We restrict our analysis here to the simplest such model where R-parity is conserved and there are universal soft breaking masses at M_G (*i.e.*, mSUGRA). Such models depend on four parameters and one sign : m_0 the universal soft breaking scalar mass at M_G; $m_{1/2}$ the universal gaugino mass at M_G. A_0 the universal cubic soft breaking mass at M_G; $\tan\beta \equiv < H_2 > / < H_1 >$ where $< H_{1,2} >$ gives rise to (d,u) quark masses, and the sign of μ, the Higgs mixing parameter which appears in the $\mu H_1 H_2$ contribution in the superpotential. (Note that the gluino mass scales approximately with $m_{1/2}$, *i.e.*, $m_{\tilde{g}} \cong 2.4\, m_{1/2}$.) No assumptions are made on the nature of the GUT group which breaks to the SM group at M_G. The model used here is the same as that used in LHC analyses by ATLAS and CMS [8,24]. Over almost all of the parameter space, the lightest neutralino ($\tilde{\chi}_1^0$) is the lightest supersymmetric particle (LSP), and is a natural candidate for cold dark matter [25].

In the present study, we fix $A_0 = 0$ and the sign of μ to be positive ($\mu > 0$) for simplicity, and choose $\tan\beta = 3$, 10, and 30. Here the ISAJET sign convention for μ [26] is used. The top quark mass is set to 175 GeV. We restrict the parameter space so that the lighter third generation squarks ($\tilde{b}_1$ and $\tilde{t}_1$) remain heavier than the lightest chargino $\tilde{\chi}_1^\pm$ and the next to lightest neutralino $\tilde{\chi}_2^0$, and also develop cuts sensitive to gluinos and squarks. These would decay to the SM particles plus the $\tilde{\chi}_1^0$. For example, $\tilde{g} \to q\bar{q}'\tilde{\chi}_1^\pm$, $\tilde{q}_L \to q'\tilde{\chi}_1^\pm$, followed by $\tilde{\chi}_1^\pm \to q\bar{q}'\tilde{\chi}_1^0$ or $\tilde{\chi}_1^\pm \to \ell^\pm\nu\tilde{\chi}_1^0$. The $\tilde{\chi}_1^0$ then would pass through the detector without interaction. Thus, the experimental signatures of pair-produced squarks and gluinos are multi jets and appreciable missing energy associated with either no lepton or some leptons. It should be noted that the event selection with a large jet multiplicity presented later in this paper is not efficient to detect the production of $\tilde{q}_R\bar{\tilde{q}}_R$, because each right chiral scalar quark dominantly decays to a quark and a $\tilde{\chi}_1^0$.

III. MONTE CARLO SIMULATION

We use ISAJET [26] for SUSY and $t\bar{t}$ events and PYTHIA [27] for all other SM processes (W/Z + jets, dibosons, QCD events) along with TAUOLA [28] and CTEQ3L parton distribution functions [29]. As for SUSY events, we generate all processes for the analyses described in Section IV. For detector simulation we use SHW [30], a simple detector simulation package developed for Run II SUSY/Higgs workshop [23]. The particle identification and misidentification efficiencies are parameterized to an expectation for Run II based on the CDF/DØ measurements at Run I in 1992-96. The SHW code provides the following objects: electron (e) with isolation, muon (μ) without isolation, hadronically decaying tau lepton (τ_h), photon (γ), jets, and calorimeter-based $\not\!\!E_T$. $\not\!\!E_T$ is the energy imbalance in the directions transverse to the beam direction using the calorimeter energies in an event [31]. We modify the SHW code to provide a muon with the isolation and the $\not\!\!E_T$ correction due to muon(s). The pseudorapidity (η) coverage is $|\eta| < 2.0$ for e and γ [23]. For μ, τ_h and tracks $|\eta|$ is < 1.5, and for jets it is < 4.0 [23]. Jets are formed with a cone size of $\Delta R \equiv \sqrt{\Delta\eta^2 + \Delta\phi^2} =$

0.4. A non-instrumented region of the detector is also simulated as a geometical acceptance for each object. (For example, SHW will reject a particular object at a rate of 10%, if the fiducial volume in a given pseudorapidity coverage is 90%.) The isolation for an electron is defined to be the calorimeter energy (excluding the electron energy) within $\Delta R = 0.4$ which is less than 2 GeV. The isolation for a muon is defined as a scalar sum of track momenta (excluding the muon momentum) within $\Delta R = 0.4$ to be less than 2 GeV. It should be noted that hadronically decaying taus (τ_h) are treated as a jet.

Throughout the paper, the leptons and jets are selected with $p_T^\ell > 15$ GeV and $E_T^j > 15$ GeV, and the reach in mass is obtained as 5σ in a significance ($\equiv N_S/\sqrt{N_B}$) for 15 fb^{-1} and 30 fb^{-1} at the Tevatron and 30 fb^{-1} at the Tripler. Here N_S (N_B) is the number of signal (background) events after a set of selection cuts.

IV. RESULTS

We consider first the jets + $\not\!\!E_T$ channel and proceed to optimize the cuts for SUSY events where $m_{\tilde{q}} \simeq m_{\tilde{g}}$. Our optimized selection is (a) $N_j \geq 6$; (b) veto on isolated leptons (e or μ); (c) $\not\!\!E_T > 200$ GeV; (d) minimum azimuthal angle between the $\not\!\!E_T$ direction and any jet $\Delta\phi^{\rm min} > 30^\circ$; (e) $M_S \equiv \not\!\!E_T + \sum_{jet} E_T^j > 1000\,{\rm GeV}$. Figure 1 shows the distributions in M_S for $t\bar{t}$, W/Z+jets, dibosons, and QCD events. The SUSY events are also superimposed in the same figure. We require in our analysis $N_S \gtrsim 30$ events. Using these cuts the total SM background is 7.0 fb (Table I).

FIGURES

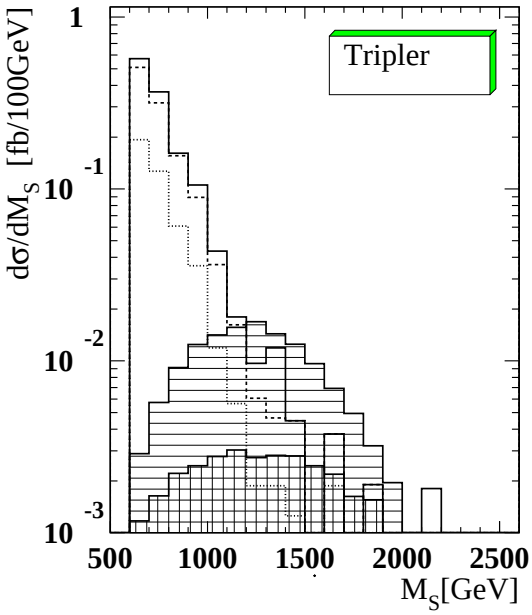

FIG. 1. Distributions of M_S for various SM processes and SUSY events with $M_S > 600$ GeV and $\not\!\!E_T > 200\,\mathrm{GeV}$ in the jets + $\not\!\!E_T$ analysis at Tripler. Dotted, dashed and solid lines are cumulative contributions from $t\bar{t}$, W/Z/dibosons, and QCD processes, respectively. Horizontally and vertically hatched histograms are for SUSY events ($\tan\beta = 3$) with $m_{\tilde{q}} \simeq m_{\tilde{g}} = 800$ GeV and 1000 GeV, respectively. The final cut on M_S is set at 1000 GeV.

Significances for SUSY events ($m_{\tilde{q}} \simeq m_{\tilde{g}}$) are plotted as function of $m_{\tilde{g}}$ in Fig. 2. We see that the reach in the gluino mass is ~ 1000 GeV (corresponding to $m_{1/2} \simeq 420$ GeV). Also there is no significant dependence between the $\tan\beta$ values of 3, 10 and 30, *i.e.*, the Tripler is sensitive to high $\tan\beta$.

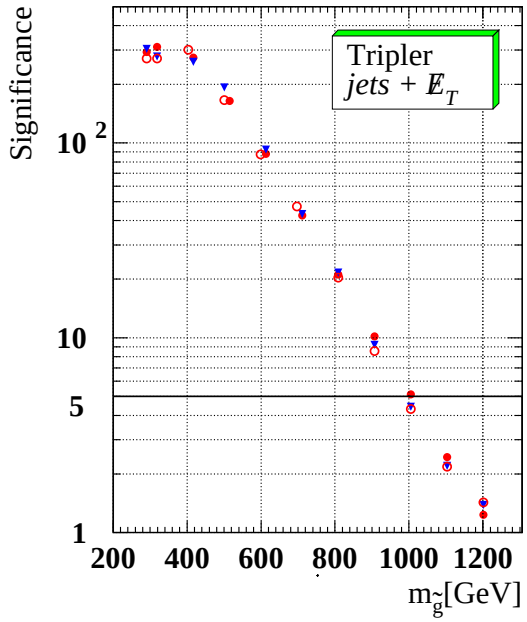

FIG. 2. Significance as a function of $m_{\tilde{g}}$ ($m_{\tilde{q}} \simeq m_{\tilde{g}}$) for $\tan\beta = 3$ (filled circles), 10 (down triangles), and 30 (open circles) in jets + $\not\!\!E_T$ channel at the Tripler.

In Fig. 3 we plot the significance as a function of m_0 at $m_{1/2} = 410$ GeV. We see that at the highest gluino mass, the Tripler is sensitive to relatively large m_0, *i.e.*, $m_0 \lesssim 450$ GeV for this channel.

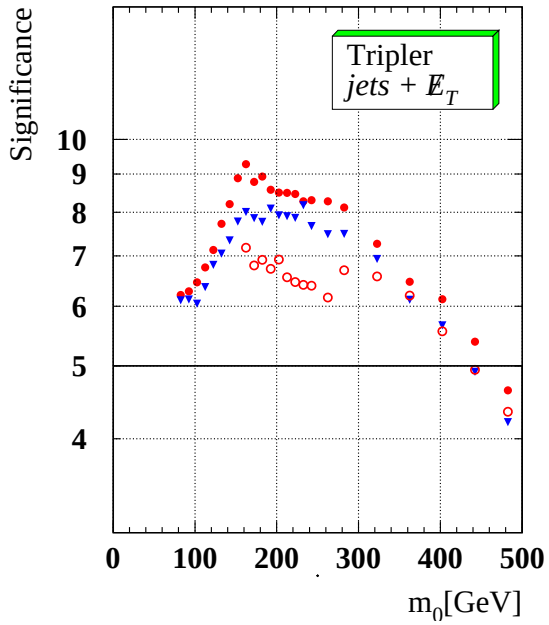

FIG. 3. Significance as a function of m_0 at $m_{1/2} = 410$ GeV ($m_{\tilde{g}} \simeq 980$ GeV) for $\tan\beta = 3$ (filled circles), 10 (down triangles), and 30 (open circles) in jets + $\not\!\!E_T$ channel at the Tripler. $m_0 \lesssim 150$ GeV is theoretically forbidden for $\tan\beta = 30$.

In Fig. 3, there are three distinct regions: (i) $m_0 \lesssim 150$ GeV, (ii) $150 \lesssim m_0 \lesssim 300$ GeV, (iii) $m_0 \gtrsim 300$ GeV. For $m_0 \gtrsim 300$ GeV, all sleptons are heavier than $\tilde{\chi}_1^\pm$ and $\tilde{\chi}_2^0$. The jet multiplicity in the SUSY events is determined by the W, Z, and light Higgs boson (h) decays in $\tilde{\chi}_1^\pm \to W\tilde{\chi}_1^0$ and $\tilde{\chi}_2^0 \to h\tilde{\chi}_1^0/Z\tilde{\chi}_1^0$, whose branching ratios are independent of m_0. Thus there is no change in the event topology, but the cross section for $\tilde{q}\bar{\tilde{q}}$ and $\tilde{g}\tilde{q}$ decrease as m_0 (*i.e.*, squark masses) increases. For $150 \lesssim m_0 \lesssim 300$ GeV, the m_0 dependence becomes somewhat gradual. This is because, as $\tilde{\tau}_1$ (and $\tilde{e}_R$) gets lighter than $\tilde{\chi}_1^\pm$, the decay mode $\chi_1^\pm \to \tilde{\tau}_1\nu$ starts competing with $\tilde{\chi}_1^\pm \to W^\pm\tilde{\chi}_1^0$. Thus the jet multiplicity in the SUSY events invloving $\tilde{\chi}_1^\pm$ decay mode is reduced to affect its event acceptance (with $N_j \geq 6$). In contrast, $\tilde{\chi}_2^0 \to \tau\tilde{\tau}_1$ decay (competing with $\tilde{\chi}_2^0 \to h\tilde{\chi}_1^0/Z\tilde{\chi}_1^0$ especially for $\tan\beta = 10$ and 30) does not alter the jet multiplicity. We notice the significance has a $\tan\beta$ dependence at a fixed m_0. This can be explained by (a) a change of the third-generation squark masses (especially the $\tilde{t}_1$), resulting in the change of squark production cross sections and (b) an enhancement of branching ratio for $\tilde{\chi}_1^\pm \to \tilde{\tau}_1\nu$ in large $\tan\beta$ region, The decay mode $\tilde{\chi}_1^\pm \to W^\pm\tilde{\chi}_1^0$ is dominant in low $\tan\beta$ region, resulting in the change of jet multiplicity. A characteristic change for $m_0 \lesssim 150$ GeV at $\tan\beta = 3$ and 10, where $\tilde{e}_L$ and $\tilde{\nu}$ become lighter than $\tilde{\chi}_1^\pm$ and $\tilde{\chi}_2^0$), is explained by a monotonic decrease of rates of $\tilde{\chi}_1^\pm \to W^\pm\tilde{\chi}_1^0$ and $\tilde{\chi}_2^0 \to h\tilde{\chi}_1^0$ decays as m_0 decreases. Thus the significance of the SUSY events with $N_j \geq 6$ is degraded.

Figure 4 gives a comparison of what might be expected at Run II at the Tevatron with 15 fb^{-1}. Our selection cuts in this case were: (a) $N_j \geq 4$; (b) veto on isolated leptons; (c) $\not\!\!E_T > 100$ GeV; (d) $\Delta\phi^{\rm min} > 30^\circ$; (e) $M_{S_2}(\equiv \not\!\!E_T + E_T^{j_1} + E_T^{j_2}) > 350$ GeV [14]. The total SM background is 73 fb (Table I).

One sees that the maximum reach for the jets $+\not\!\!E_T$ channel in Fig. 4 is 410 GeV in gluino mass, which rises to 440(460) GeV for 15(30) fb^{-1} of data when $m_{\tilde{q}} < m_{\tilde{g}}$. (These results are consistent with previous Tevatron studies [13,16].) The latest bound on the $\tilde{\chi}_1^\pm$ mass of $\gtrsim 103$ GeV from LEPII [32] requires $m_{\tilde{g}} \gtrsim 420$ GeV, since we have $m_{\tilde{\chi}_1^\pm} \simeq m_{\tilde{g}}/3$ from gaugino unification. In addition, one may show that Run II will also be able to sample limited range of m_0, *i.e.*, for $m_0 \lesssim 200$ GeV for $m_{\tilde{g}} = 420$ GeV. Thus there is a significant

improvement in going from the Tevatron to the Tripler.

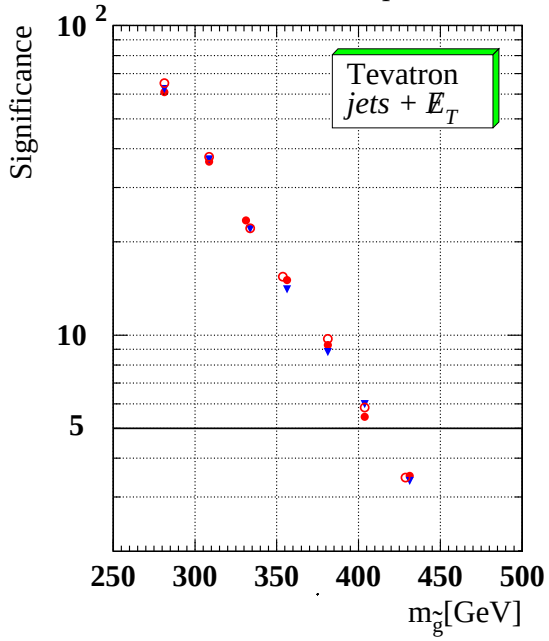

FIG. 4. Significance for 15 fb^{-1} of luminosity as a function of $m_{\tilde{g}}$ ($m_{\tilde{q}} \simeq m_{\tilde{g}}$) for $\tan\beta = 3$ (filled circles), 10 (down triangles), and 30 (open circles) in jets + $\not\!\!E_T$ channel at the Tevatron.

We consider next the 1ℓ + jets + $\not\!\!E_T$ channel. This channel gives the largest reach for the LHC, and we will see that there are regions of SUSY parameter space where the discovery reach for gluinos is also improved. Here we select events with (a) $N_j \geq 4$; (b) $N_\ell = 1$; (c) $\not\!\!E_T > 200$ GeV; (d) $\Delta\phi^{\rm min} > 30^\circ$; (e) $M_T (\equiv \sqrt{2\not\!\!E_T p_T^\ell [1 - \cos\Delta\phi(\ell, \not\!\!E_T)]}) > 160$ GeV; (f) $M_S > 600$ GeV. The M_T cut is applied to remove W events. The SM background is 0.32 fb (Table I).

In Fig. 5, we compare the m_0 dependence of the significance for $\tan\beta = 3$, 10 and 30 at $m_{1/2} = 410$ GeV ($m_{\tilde{g}} \simeq 980$ GeV). We see here the m_0 reach is not as large as in the jets + $\not\!\!E_T$ channel. In this parameter space, the $\tilde{\ell}_L$ and the $\tilde{\nu}$ are lighter than the $\tilde{\chi}_1^\pm$ and the $\tilde{\chi}_2^0$ when $m_0 \lesssim 150$ GeV. Thus, the branching ratios of $\tilde{\chi}_1^\pm \to \ell\tilde{\nu}$ ($\tilde{\ell}_L\nu$) and $\tilde{\chi}_2^0 \to \ell\tilde{\ell}$ increase as m_0 decreases, and the significance in the 1ℓ + jets + $\not\!\!E_T$ channel is improved dramatically and is significantly higher than for the jets + $\not\!\!E_T$ channel (See Fig. 3). An interesting feature occurs at $m_0 \simeq 140$ GeV which distinguishes between the $\tan\beta = 3$ and 10 scenarios. The SUSY particle masses for these two $\tan\beta$ values are very close, except for the $\tilde{\tau}_1$ mass. The

$\tilde{\tau}_1$ mass at $\tan\beta = 10$ is lighter, so that the branching ratios of $\tilde{\chi}_1^{\pm} \to \tilde{\tau}_1 \nu$ and $\tilde{\chi}_2^0 \to \tau\tilde{\tau}_1$ are larger to decrease the 1ℓ + jets + $\not\!\!E_T$ signature.

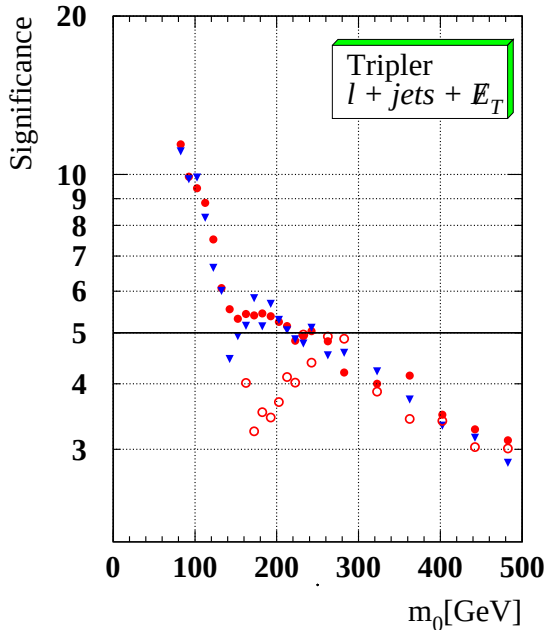

FIG. 5. Same as in Fig. 3 ($m_{1/2}$ = 410 GeV), but in 1ℓ + jets + $\not\!\!E_T$ channel.

As before, for comparison, we show the significance for $m_{1/2} = 160$ GeV in this channel for the Tevatron in Fig. 6. The event selections for this figure was made with the following cuts: (a) $N_j \geq 2$; (b) $N_\ell = 1$; (c) $\not\!\!E_T > 40$ GeV; (d) $\Delta\phi^{\rm min} > 30^\circ$; (e) $M_T < 50$ GeV or > 110 GeV; (f) $M_{S_2} > 350$ GeV. The M_T cut is applied to remove W events. The SM background size is 70 fb (Table I). The significance is found to be always below 5σ for the entire region of parameter space.

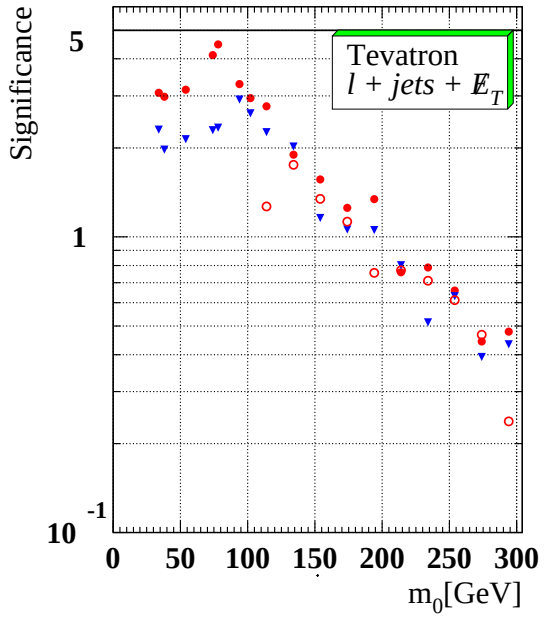

FIG. 6. Significance for 15 fb^{-1} of luminosity as a function of m_0 for $\tan\beta = 3$ (filled circles), 10 (down triangles), and 30 (open circles) in 1ℓ + jets + $\not\!\!E_T$ channel at the Tevatron for $m_{1/2} = 160$ GeV ($m_{\tilde{g}} \simeq 420$ GeV).

From Figs. 3 and 5, the significance in jets + $\not\!\!E_T$ and 1ℓ + jets + $\not\!\!E_T$ channels appear to be maximized at $m_0 = 140$-160 GeV and 100 GeV respectively, for $m_{1/2} = 410$ GeV. To obtain the strongest reaches we therefore systematically scan mSUGRA points at $\tan\beta = 3$ for $m_{1/2} = \{360, 400, 440, 470, 500, 540\}$ GeV and $m_0 = \{100, 140, 180, 220, 260\}$ GeV. Figure 7 shows significance as a function of the gluino mass in both jets + $\not\!\!E_T$ (hatched region bounded by the dashed lines) and 1ℓ + jets + $\not\!\!E_T$ (region bounded by the dotted lines) analyses for the above mSUGRA points. We see that the strongest reach in the jets + $\not\!\!E_T$ channel is $m_{\tilde{g}} \simeq 1060$ GeV ($m_{1/2} \simeq 440$ GeV) and $m_{\tilde{g}} \simeq 1140$ GeV ($m_{1/2} \simeq 480$ GeV) in the 1ℓ + jets + $\not\!\!E_T$ channel. The dot-dashed line represents jets + $\not\!\!E_T$ channel for m_0= 650 GeV and $\tan\beta = 3$. Even for this large m_0, we can see that the 5σ significance can be achieved for $m_{\tilde{g}} \simeq 900$ GeV ($m_{\tilde{q}_{1,2}} \simeq 970$ GeV, where $m_{\tilde{q}_{1,2}}$ are the squark masses of the first two generations).

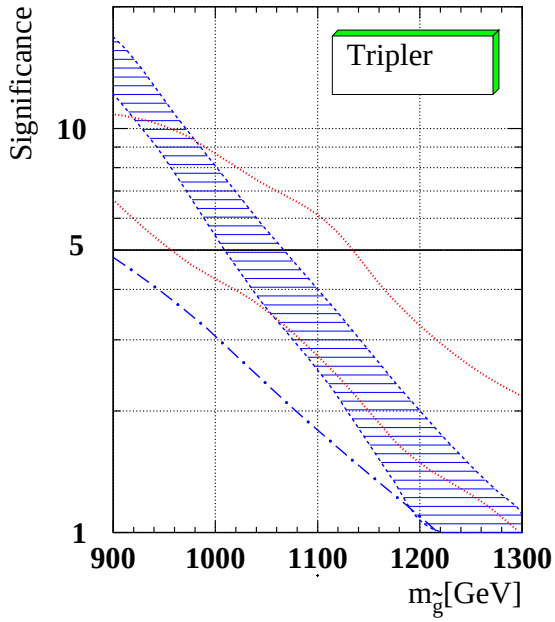

FIG. 7. Significance as a function of $m_{\tilde{g}}$ for $\tan\beta = 3$ in jets + $\not\!\!E_T$ (hatched region bounded by the dashed lines) and 1ℓ + jets + $\not\!\!E_T$ (region bounded by the dotted lines) channels at the Tripler. Ranges scanned are $360 \leq m_{1/2} \leq 540$ GeV and $100 \leq m_0 \leq 260$ GeV. The dot-dashed line represents jets + $\not\!\!E_T$ channel for m_0= 650 GeV and $\tan\beta = 3$.

V. CONCLUSION

We have studied the signals for gluinos and squarks within the framework of mSUGRA models in the jets + $\not\!\!E_T$ and 1ℓ + jets + $\not\!\!E_T$ channels for the Tripler $p\bar{p}$ accelerator with $\sqrt{s} = 5.4$ TeV. The Tripler would have a maximum reach of $m_{\tilde{g}} \simeq 1140$ GeV with 30 fb^{-1} in the 1ℓ + jets + $\not\!\!E_T$ channel (for $m_0 \simeq 100$ GeV, $\tan\beta$=3-10) and $m_{\tilde{g}} \simeq 1060$ GeV in the jets + $\not\!\!E_T$ channel (for $140 \lesssim m_0 \lesssim 200$ GeV, $\tan\beta = 3$). This gluino mass reach is comparable to the Tripler's reach of 380 GeV chargino (with 40 fb^{-1}) in the trilepton channel [7] via direct chargino-neutralino ($\tilde{\chi}_1^{\pm}$-$\tilde{\chi}_2^0$) production, since gaugino unification implies $m_{\tilde{\chi}_1^{\pm}} \simeq m_{\tilde{g}}/3$. The above results can be compared with 440(460) GeV for the jets + $\not\!\!E_T$ channel for 15(30) fb^{-1} of luminosity at the Tevatron. For $m_{\tilde{g}} \simeq 980$ GeV, the Tripler covers relatively large values of m_0, *i.e.*, to $m_0 \lesssim 420$ GeV in the jets + $\not\!\!E_T$ channel. Note also, from Figs. 2 and 3, that this gluino and m_0 reach of the Tripler is valid for large tanβ while the trilepton analysis [7]

is sensitive only for small tanβ (*e.g.*, tanβ=3).

In the above analysis we have set A_0=0. The results for the maximum Tripler reach are not very sensitive to A_0. Thus there is almost no change for $A_0 > 0$ and for $A_0 = -1000$ GeV, tanβ=3, the gluino reach is increased by about 20 GeV in the 1ℓ + jets + $\not\!\!E_T$ channel.

In SUGRA models of this type, the $\tilde{\chi}_1^0$ is the LSP and hence is the main candidate for cold dark matter. The astronomical constraints on the amount of relic neutralinos generally implies $m_0 \lesssim 200$ GeV, for $m_{1/2} \lesssim$ 350-400 GeV. For higher $m_{1/2}$, coannihilation effects dominate [33] and for high $\tan\beta$, m_0 can rise to $\lesssim$ 400-500 GeV [34]. Thus the Tripler would be sensitive to much of the cosmologically interesting part of the parameter space.

The LHC gluino reach is $m_{\tilde{g}} \lesssim 2.5$ TeV [8,24], which is much higher than the Tripler. The Tripler is however complementary to the LHC in that the production of squarks and gluinos go in part through different channels, as are the detector signals for the charginos and neutralinos. Thus provided SUSY lies sufficiently low to be seen at the Tripler, the two accelerators would be sensitive to different supersymmetric interactions.

ACKNOWLEDGEMENTS

We thank Muge Karagoz for her participation in the earlier stage of our analysis. This work was supported in part by DOE grant Nos. DE-FG03-95ER40917, DE-FG03-95ER40924 and NSF grant No. PHY-9722090.

REFERENCES

[1] P. McIntyre, E. Accomando, R. Arnowitt, B. Dutta, T. Kamon, and A. Sattarov, hep-ex/9908052 (1999).

[2] R. Gupta, "Common Coil Magnet System for VLHC," Proc. of 1999 Part. Acc. Conf., New York, p.3239 (1999).

[3] G. Ambrosio *et al.*, "Conceptual Design of the Fermilab Nb_3Sn High Field Dipole Model,"Proc. of 1999 Part. Acc. Conf., New York, p. 174 (1999).

[4] K. Chow *et al.*, "Fabrication and Test Results of a Nb_3Sn Superconducting Racetrack Dipole Magnet,"Proc. of 1999 Part. Acc. Conf., New York, p. 171 (1999).

[5] C. Battle *et al.*, "Optimization of Block-coil Dipoles for Hadron Colliders,"Proc. of 1999 Part. Acc. Conf., New York, p. 2936 (1999).

[6] American Linear Collider Working Group (J. Bagger *et al.*), "The Case for a 500-GeV e^+e^- Linear Collider," hep-ex/0007022 (2000).

[7] V. Barger, K. Cheung, T. Han, C. Kao, T. Plehn, R-J. Zhang, Phys. Lett. B **478**, 224 (2000).

[8] ATLAS: Detector and Physics Performance Technical Design Report, vol. 1, CERN-LHCC-99-14, ATLAS-TDR-14 (1999); vol. 2, CERN-LHCC-99-15, ATLAS-TDR-15 (1999).

[9] K. Lassila-Perini,"Discovery Potential of the Standard Model Higgs in CMS at the LHC," CERN-THESIS-99-3(1998).

[10] U.M. Heller, M. Klomfass, H. Neuberger, and P. Vranas, Nucl. Phys. B **405**, 555 (1993).

[11] For reviews on SUSY and the MSSM, see *e.g.*, H.P. Nilles, Phys. Rep. **110**, 1 (1984) and H.E. Haber and G.L. Kane, Phys. Rep. **117**, 75 (1995).

[12] A.H. Chamseddine, R. Arnowitt, and P. Nath, Phys. Rev. Lett. **49**, 970 (1982); R. Bar-

bieri, S. Ferrara, and C.A. Savoy, Phys. Lett. B **119**, 343 (1982); L. Hall, J. Lykken, and S. Weinberg, Phys. Rev. D **27**, 2359 (1983). For a review, see R. Arnowitt and P. Nath, Nucl. Phys. B **227**, 121 (1983).

[13] H. Baer, C.-H. Chen, C. Kao, and X. Tata, Phys. Rev. D **52**, 1565 (1995); H. Baer, C. Chen, F. Paige, and X. Tata, *ibid.* **54**, 5866 (1996).

[14] S. Mrenna, G.L. Kane, G.D. Kribs, and J.D. Wells, Phys. Rev. D **53**, 1168 (1996).

[15] TeV2000 Group, "Future ElectroWeak Physics at the Fermilab Tevatron: Report of the TeV2000 Study Group," *eds.* D. Amidei and R. Brock, Fermilab-Pub-96/082 (1996).

[16] H. Baer, C.-H. Chen, M. Drees, F. Paige, and X. Tata, Phys. Rev. Lett. **79**, 986 (1997); *ibid.* **80**, 642 (1998) (E); Phys. Rev. D **58**, 075008 (1998).

[17] V. Barger, C. Kao, and T-J. Li, Phys. Lett. B **433**, 328 (1998); V. Barger and C. Kao, Phys. Rev. D **60**, 115015 (1999).

[18] H. Baer, M. Drees, F. Paige, P. Quintana, and X. Tata, Phys. Rev. D **61**, 095007 (2000).

[19] K.T. Matchev and D.M. Pierce, Phys. Rev. D **60**, 075004 (1999); Phys. Lett. B **467**, 225 (1999); J.D. Lykken and K.T. Matchev, Phys. Rev. D **61**, 015001 (2000).

[20] E. Accomando, R. Arnowitt, and B. Dutta, Phys. Lett. B **475**, 176 (2000).

[21] G. Anderson, H. Baer, C.-H. Chen, and X. Tata, Phys. Rev. D **61**, 095005 (2000).

[22] R. Demina, J.D. Lykken, K.T. Matchev, and A. Nomerotski, Phys. Rev. D **62**, 035011 (2000).

[23] S. Abel *et al.*, "Report of the SUGRA Working Group For Run II of the Tevatron," hep-ph/0003154 (2000).

[24] CMS Collaboration, S. Abdullin *et al.*, "Discovery Potential for Supersymmetry in CMS," hep-ph/9806366 (1998).

[25] H. Goldberg, Phys. Rev. Lett. **50**, 1419 (1983); J. Ellis, J.S. Hagelin, D.V. Nanopoulos, K. Olive, and M. Srednicki, Nucl. Phys. B **238**, 453 (1984).

[26] H. Baer, F. Paige, S.D. Protopopescu, and X. Tata, "ISAJET 7.48: A Monte Carlo Event Generators for pp, $\bar{p}p$, and e^+e^- Reactions," hep-ph/0001086 (2000).

[27] T. Sjöstrand, Commput. Phys. Commun. **82**, 74 (1994); T. Sjostrand, P. Eden, C. Friberg, L. Lonnblad, G. Miu, and S. Mrenna, hep-ph/0010017 (2000).

[28] S. Jadach, J.H. Kühn, and Z. Wąs, Commput. Phys. Commun. **64**, 275 (1991); M. Jeżabek, Z. Wąs, S. Jadach, and J.H. Kühn, *ibid.* **70**, 69 (1992); S. Jadach, Z. Wąs, R. Decker, and J.H. Kühn, *ibid.* **76**, 361 (1993). We use version 2.5.

[29] CTEQ Collaboration, H. L. Lai *et al.*, Phys. Rev. D **51**, 4763 (1995).

[30] J. Conway, "User's Guide to the SHW Package," http://www.physics.rutgers.edu/~jconway/soft/shw/shw.html. We use version 2.3 with StdHep (version 4.06 - http://www-pat.fnal.gov/stdhep.html) and CERNLIB 2000.

[31] In the CDF/DØ coordinate system, θ and ϕ are the polar and azimuthal angles with respect to the proton beam direction.

[32] I. Trigger, OPAL Collaboration, talk presented at the DPF 2000, Columbus, OH; T. Alderweireld, DELPHI Collaboration, talk presented at the DPF 2000, Columbus, OH.

[33] J. Ellis, A. Ferstl, and K. A. Olive, Phys. Lett. B **481**, 304 (2000).

[34] R. Arnowitt, B. Dutta, and Y. Santoso, hep-ph/0010244 (2000).

TABLES

TABLE I. The background cross sections in fb (after cut) of jets + $\not{E}_T$ and 1ℓ + jets + $\not{E}_T$ channels. Cuts are specified in the text.

	Tripler		Tevatron	
Process	jets + $\not{E}_T$	1ℓ + jets + $\not{E}_T$	jets + $\not{E}_T$	1ℓ + jets + $\not{E}_T$
$t\bar{t}$	2.5	0.06	25	14
W+jets	1.1	0.21	23	48
Z+jets	1.2	0.05	15	6
diboson	0.0	0.0	1	2
QCD	2.2	0.0	9	0.0
Total	7.0	0.32	73	70